

PRODUCTION OF ROD-LIKE MORPHOLOGY OF $\text{Cu}_3(\text{BTC})_2$ METAL-ORGANIC FRAMEWORKS USING ONE MINUTE SONICATION

Data de aceite: 01/06/2021

Data de submissão: 05/04/2021

Aline Geice Silva de Oliveira

Universidade Federal de Minas Gerais,
Departamento de Engenharia Metalúrgica e de
Materiais
Belo Horizonte – Minas Gerais
<http://lattes.cnpq.br/2028657699989569>

Daniela Cordeiro Leite Vasconcelos

Universidade Federal de Minas Gerais,
Departamento de Engenharia Metalúrgica e de
Materiais
Belo Horizonte – Minas Gerais
<http://lattes.cnpq.br/3281433683051375>

Peter George Weidler

Karlsruhe Institute of Technology, Institute of
Functional Interfaces
Karlsruhe – BW, Germany
https://www.ifg.kit.edu/english/21_215.php

Wander Luiz Vasconcelos

Universidade Federal de Minas Gerais,
Departamento de Engenharia Metalúrgica e de
Materiais
Belo Horizonte – Minas Gerais
<http://lattes.cnpq.br/3617697065989200>

ABSTRACT: This paper reports a new short time strategy for producing rod-like morphology of metal-organic frameworks (MOFs), by using one minute ultrasonic homogenizer (or “sonicator”) at room temperature and ambient pressure. The crystallinity of the obtained $\text{Cu}_3(\text{BTC})_2$ was

investigated by X-ray diffraction and its stable formation corroborated with Fourier transform infrared spectroscopy (FTIR) results. This study promotes an optimization process to synthesize MOFs.

KEYWORDS: Metal-organic frameworks (MOF), Morphology, Ultrasonic Energy, X-Ray Diffraction, FTIR Spectroscopy.

PRODUÇÃO DE REDES TRIDIMENSIONAIS ORGANOMETÁLICAS (MOFS) DO TIPO $\text{Cu}_3(\text{BTC})_2$ COM MORFOLOGIA DE BASTONETES USANDO SONICAÇÃO POR APENAS UM MINUTO

RESUMO: Este artigo demonstra uma nova estratégia para a produção rápida de estruturas metal-orgânicas (MOFs) com morfologia de bastonete, usando um homogeneizador ultrassônico (ou “sonicador”) por um minuto em temperatura e pressão ambientes. A cristalinidade do MOF $\text{Cu}_3(\text{BTC})_2$ obtido foi investigada por Difração de Raios X e sua estabilidade foi corroborada com os resultados de Espectroscopia FTIR (Fourier Transform Infrared Spectrometer). Este estudo contribui para a otimização do processo de síntese dos MOFs.

PALAVRAS - CHAVE: Redes tridimensionais organometálicas (MOF), Morfologia, Energia ultrassônica, Difração de raios X, Espectroscopia FTIR.

1 | INTRODUCTION

Metal-organic frameworks (MOFs) are crystalline and porous materials with chemical flexible properties which are composed of transition metals ions or clusters linked by organic ligands (Domán et al.; Tranchemontagne et al.). They present wide applications, such as gas storage and separation (Zhao et al.; Valadez Sánchez et al.; Shan et al.), catalysis (Remya and Kurian), carbon dioxide capture (Trickett et al.), among others (Fischer and Bétard; Kayal et al.). In this sense, researches have been done to improve its synthesis parameters (T. Chen et al.; Moosavi et al.). The metal-organic framework $\text{Cu}_3(\text{BTC})_2$, a coordination compound formed by copper and trimesic acid, also known as Cu-BTC and HKUST-1, is one of the widely studied MOF.

Several methods are applied in Cu-BTC synthesis, such as sonochemical, solvothermal, electrochemical and microwave (Furukawa et al.). The sonochemical procedure, in particular, has been noted in the last years (Li et al.; Xu et al.), although some ultrasonic machines offer dispersed energy, which difficult the synthesis of the material (Sargazi et al.; da Silva et al.). This suggests the necessity to discover new routes to achieve an increase in the yield of produced MOFs and reductions of the synthesis time. In this scenario, the sonicator has been recently used to obtain the Cu-BTC MOF and varied morphologies (Israr et al.; Luo et al.; Dhumal et al.). In this study, we produced a rod-like Cu-BTC and presented an optimized synthesis through ultrasonic homogenizer (or “sonicator”).

2 | EXPERIMENTAL

2.1 CuBTC preparation

The $\text{Cu}_3(\text{BTC})_2$ DMF-based was prepared using copper acetate anhydride ($\text{Cu}(\text{OAc})_2$), 1,3,5-benzene tricarboxylic acid (H_3BTC), and ethanol (99.5%), used without further purification. All the reagents were purchased by Sigma-Aldrich. The H_3BTC was dissolved in 25 mL N,N-dimethylformamide (DMF 99,8%) and cupric acetate was added in the same solution. Then ultrasonic irradiation was applied at different reaction times. The mixture was filled in a 50 mL vessel and heated to 120 °C for 12 h, within and without autoclave to compare. The products were filtered, washed with ethanol and dried at 60 °C.

2.2 Ultrasonic radiation interference experiments

During the ultrasonic irradiation cited step, the reaction times were varied from 1 min to 60 min at a frequency of 24 KHz and 60% of power (UP 200S, Hielscher Ultrasonics GmbH, Teltow, Germany), called in this work “sonicator”, output 200W, Figure 1, Sonotrode S3. The time was varied to find the necessary minimum time to obtain the material.

2.3 Techniques used for characterization

The materials were characterized by powder X-ray diffractometer (XRD) PANalytical Empyrean X-ray in the 2θ range from 5° to 20° , using scan speed of 0.02° with an acquisition time of 20s per step. Due to the anisotropic shape of the particles, preferential orientation was checked with the help of the Williamson-Hall approach (G.K. Williamson and W.H. Hall). FTIR spectroscopy (Perkin-Elmer Frontier spectrometer with aid of ATR accessory) was performed between 4000 cm^{-1} and 400 cm^{-1} , with a resolution of 4 cm^{-1} and 128 scans. Scanning electron microscope (SEM) Quanta 3D FEG FEI was used for morphologies analyses. To perform the analysis on the SEM, the samples were powdered and their surfaces were covered with a layer of about 15 nm of amorphous carbon to improve surface conductivity, avoiding the accumulation of charges during image acquisition. TEM images were obtained from transmission electron microscope G2-20-SuperTwin FEI microscope. Thermal analyses (TGA) were measured using a Perkin-Elmer STA 6000 simultaneous thermal analyzer Instrument in N_2 atmosphere. The materials were heated from $30\text{ }^\circ\text{C}$ to $900\text{ }^\circ\text{C}$ at a rate of $10\text{ }^\circ\text{C} / \text{min}$.

3 | RESULTS AND DISCUSSION

In this study we use an ultrasonic homogenizer (or “sonicator”) that works both directly through cavitation energy transfer mechanism, whereby bubbles form and collapse, as well as through the ultrasonic forces, by introducing a probe into the sample, as shown in Fig. 16. The probe vibrates rapidly and transfers its ultrasonic energy to the sample with a more localized process, which provides uniform MOFs in just a few seconds (da Silva et al.; Li et al.; Sargazi et al.).

Ultrasound is cyclic mechanical vibration between 20 kHz and 10 MHz. It can interact with liquids, alternating areas of compression (high pressure) and rarefaction (low pressure). In the low pressure region small bubbles are formed. The bubbles grow (tens of micrometers) under alternating pressure and ultrasonic energy is accumulated. When the bubbles reach their maximum size, they become unstable and collapse: cavitation process. Rapid energy release with heating and cooling rates of 10^{10} K/s , temperatures around 5000 K and pressures of around 1000 bar. Thereby, these points present very unusual conditions of short duration and extremely high temperatures and pressures inside the collapsing bubble and nearby (ring of $\pm 200\text{ nm}$) (Stock and Biswas).

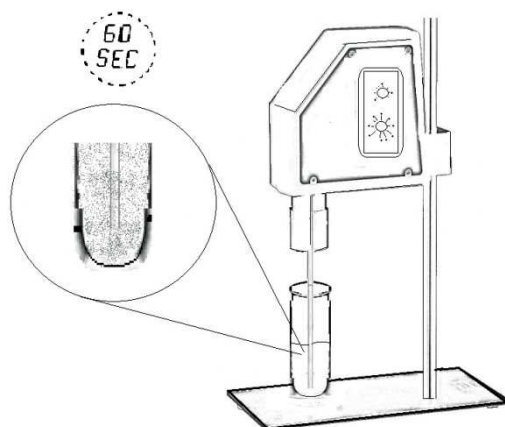


Figure 1. Illustration of the dispersion of nanoparticles by using high energy ultrasonic homogenizer to MOF preparation

In this way, the Cu-BTC MOFs were prepared by using copper acetate and H_3BTC in DMF under sonicator for only 1 min, at room temperature and ambient pressure, (Figure 2a) which was enough to obtain a high amount of $Cu_3(BTC)_2$ (68,5%, based on Cu). Furthermore, combining with the solvothermal method, by using autoclave, we achieved even higher values of $Cu_3(BTC)_2$ (78,1%, based on Cu), Figure 2b and after the drying process Figure 2c.

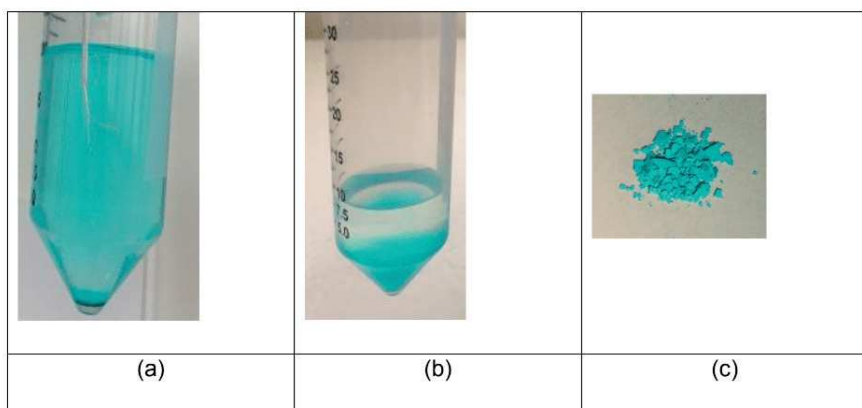


Figure 2. Process of obtaining MOFs: (a) mixture of copper and BTC precursors, (b) separation of the two phases (MOF and solvent) characteristic of the formation of the MOF and (c) final MOF powder.

3.1 XRD

The Figure 3 shows the XRD patterns of the resulting MOFs obtained by using sonicator even at very low times. The results for the samples obtained using one and five minutes of sonication were evaluated and compared with the literature. In this sense, all of the diffraction peaks could be correlated to the crystalline $\text{Cu}_3(\text{BTC})_2$ pattern (ref.(Schlichte et al.; Chui et al.)). The absence of additional peaks in the presented range demonstrates a satisfactory level of purity of the crystalline structure. In addition, reflections of an unknown phase appear (not shown here) when the reaction time was increased to 30 min, 60 min and 120 min, indicating that the structure of the sample is changed due to ultrasound irradiation for a long reaction time, as suggested by the results for the five minutes sample shown at Figure 2. Furthermore, the yield of solvent into the MOF pores may interfere in the relative intensities of the diffraction peaks (Li et al.; da Silva et al.). From the Williamson-Hall plot applying all observed (hkl)-reflections, no anisotropy could be deduced. Thus, the shape of the particles is not reflected in the crystalline domains. Their size was calculated from the plot to 23 nm and the stress/strain parameter ϵ_0 to 0.0021 d_0/d , with d the lattice plane distance. These results indicated that fast sonicator dispersion of the particles allows the formation of crystalline and well-defined structures, which is consistent with results obtained from FTIR.

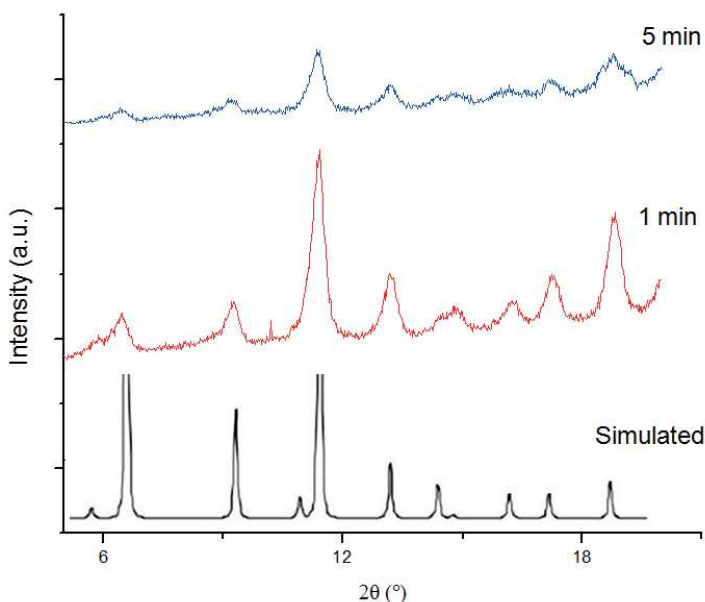


Figure 3. Powder X-Ray diffraction patterns simulated from the crystallographic data of $\text{Cu}_3(\text{BTC})_2$ (ref. (Chui et al.)), and samples synthesized by using high energy sonicator: 1 min and 5 min.

3.2 FTIR

The FTIR spectrum illustrated in Figure 4 shows the comparison between the synthesized $\text{Cu}_3(\text{BTC})_2$ and H_3BTC , source of BTC. The bands around 1634 cm^{-1} , 1446 cm^{-1} , 1419 cm^{-1} and 1372 cm^{-1} refer to the pure Cu-BTC which are attributed to vibrations of its carboxylate group. The 1634 and 1419 cm^{-1} founded bands were attributed to asymmetric $\nu(\text{COO})$ and symmetric $\nu(\text{COO})$ stretching modes, respectively. These modes can be assigned to those carboxylate groups located in the big pores of Cu-BTC. Meanwhile, the 1446 , and 1372 cm^{-1} peaks were attributed to asymmetric $\nu(\text{COO})$ and symmetric $\nu(\text{COO})$ stretching vibrations of those carboxylate groups located in the smaller pores (Dhumal et al.; C. Chen et al.; Liao et al.).

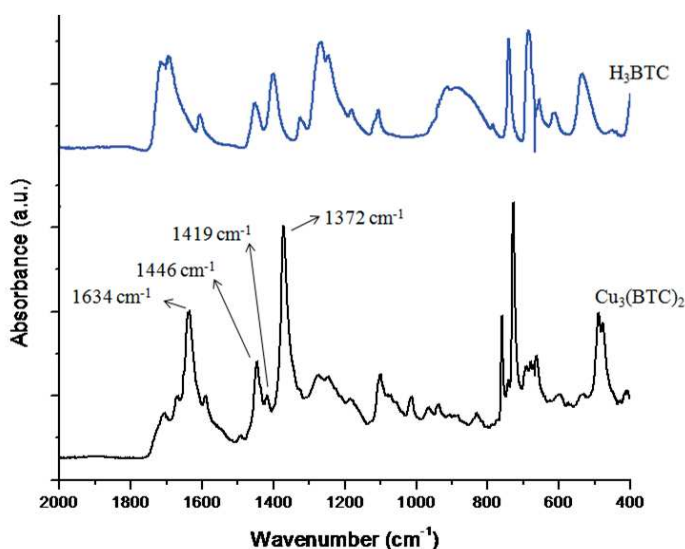


Figure 4. FTIR spectrum of H_3BTC and $\text{Cu}_3(\text{BTC})_2$ sample synthesized by 1 min ultrasonic homogenizer

3.3 Thermogravimetric analysis TG/Degradation

The obtained material was studied in terms of thermal stability by using TG/DTG analysis. The curves of Cu-BTC are shown in Figure 5. The first region showed a weak peak around $100\text{ }^\circ\text{C}$ which was related to the small presence of water that was physically adsorbed in the pores. The second region about $150\text{ }^\circ\text{C}$ suggests the loss of residual DMF and ethanol solvents. The third region of weight loss occurred around $330\text{ }^\circ\text{C}$, may be associated with the decomposition of the BTC ligands and secondary building units in Cu-BTC, which indicates a complete collapse and degradation of the MOF structure.

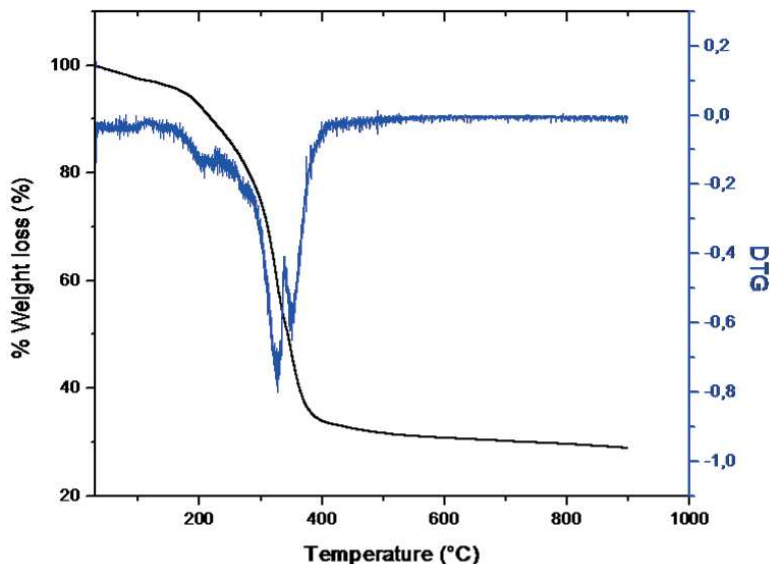


Figure 5. TG/DTG of $\text{Cu}_3(\text{BTC})_2$ sample synthesized with ultrasonic homogenizer

3.4 SEM and TEM

The SEM and TEM images shown in Figure 6 demonstrated the morphologies of the $\text{Cu}_3(\text{BTC})_2$ prepared by using 1 min sonication method. The morphologies features of rod-like are shown in Figure 6a, with a size range of 1–2 μm . According to the literature, the conventional solvothermal method presented MOFs with octahedral shape and crystal sizes in the order of nanometers, which were smaller than those found here (Li et al.; Furukawa). The crystal size can also be tuned through the reaction conditions. When the reaction was conducted using the same sonication process, although at ambient pressure, Figure 6b, the rod-like appeared more agglomerated, suggesting the formation of interconnected hollow regions. Figure 6c and d well indicated the crystalline nature of the nanomaterials by transmission electron microscope (TEM). These images corroborated the morphologies presented above with a size around 1.4 μm , and exhibited the regular rod-like morphology with hexagonal-shaped transversal section with the diameter around 100 nm, respectively. This indicated that using even few seconds of homogenizing ultrasonic irradiation, the rod-like morphology of Cu-BTC can be achieved and modeled.

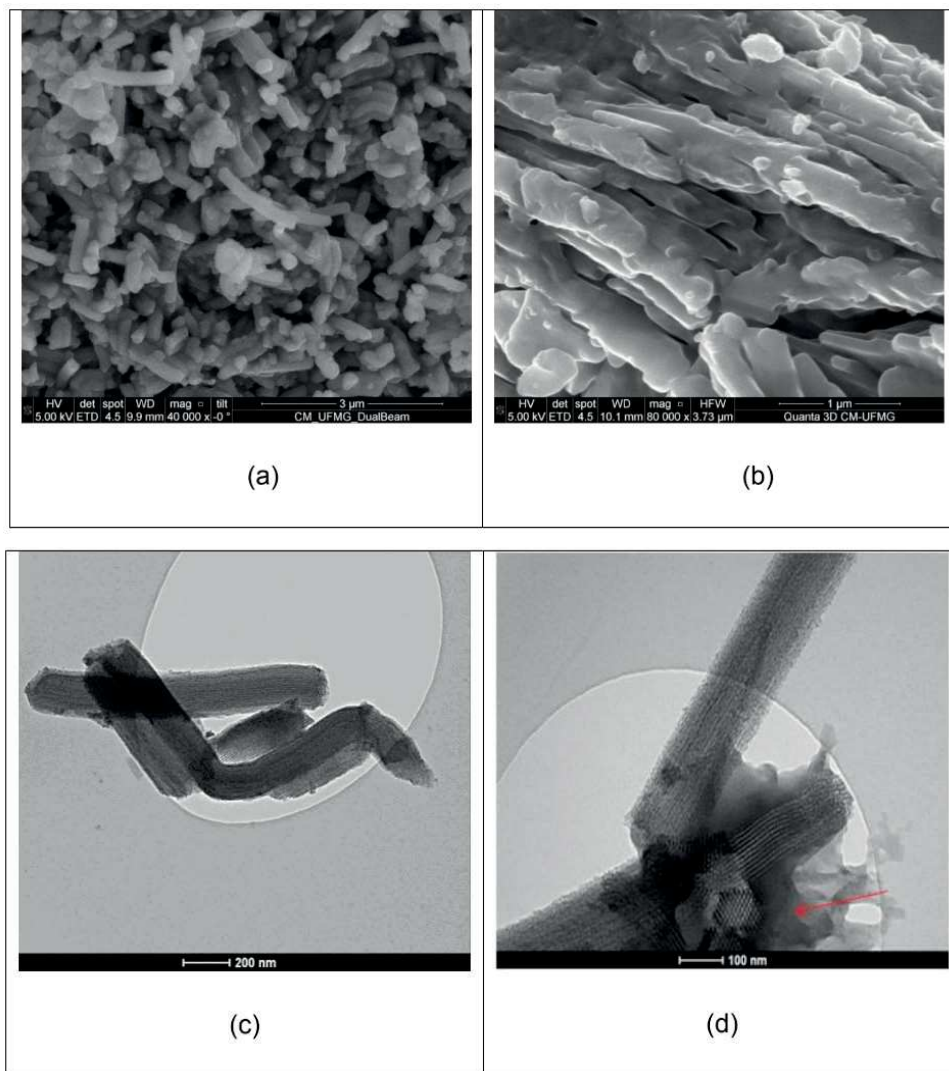


Figure 6. SEM images of Cu-BTC by one minute ultrasonic irradiation homogenizer under different pressures (a) autoclave, (b) ambient pressure; and TEM images of Cu-BTC by one minute ultrasonic irradiation homogenizer both (c) and (d) under autoclave.

4 | CONCLUSIONS

In summary, the obtained results in this study confirmed the successful rapid ultrasonic homogenization technique to rod-like $\text{Cu}_3(\text{BTC})_2$ formation. The material could be prepared by using one minute sonication method due its rapidly probe vibration and the ultrasonic energy transference. This more localized process provided uniform MOFs even at room temperature and ambient pressure. In addition, the studied homogenization step

promoted an optimization process of the MOF synthesis and could be associated with the as solvothermal and sonochemical conventional methods.

ACKNOWLEDGMENTS

The authors would like to thank the financial support of CAPES-PROEX, CNPq and FAPEMIG and, additionally, to the Institute of Functional Interfaces of the Karlsruhe University for technical support.

REFERENCES

Chen, Chong, et al. **"Synthesis of Hierarchically Structured Hybrid Materials by Controlled Self-Assembly of Metal-Organic Framework with Mesoporous Silica for CO₂ Adsorption."** ACS Applied Materials and Interfaces, vol. 9, no. 27, 2017, pp. 23060–71, doi:10.1021/acsami.7b08117.

Chen, Tian, et al. **"A Novel Hexagonal Prism Cu-BTC by Unipolar Pulse Electropolymerization."** Materials Letters, vol. 254, Elsevier B.V., 2019, pp. 137–40, doi:10.1016/j.matlet.2019.07.046.

Chui, Stephen S. Y., et al. **"A Chemically Functionalizable Nanoporous Material [Cu₃(TMA)₂(H₂O)₃](N)."** Science, vol. 283, no. 5405, 1999, pp. 1148–50, doi:10.1126/science.283.5405.1148.

da Silva, Gilvaldo G., et al. **"Sonoelectrochemical Synthesis of Metal-Organic Frameworks."** Synthetic Metals, vol. 220, no. October, Elsevier B.V., 2016, pp. 369–73, doi:10.1016/j.synthmet.2016.07.003.

Dhumal, Nilesh R., et al. **"Molecular Interactions of a Cu-Based Metal-Organic Framework with a Confined Imidazolium-Based Ionic Liquid: A Combined Density Functional Theory and Experimental Vibrational Spectroscopy Study."** Journal of Physical Chemistry C, vol. 120, no. 6, 2016, pp. 3295–304, doi:10.1021/acs.jpcc.5b10123.

Domán, Andrea, et al. **"In Situ Evolved Gas Analysis Assisted Thermogravimetric (TG-FTIR and TG/DTA-MS) Studies on Non-Activated Copper Benzene-1,3,5-Tricarboxylate."** Thermochimica Acta, vol. 647, Elsevier B.V., 2017, pp. 62–69, doi:10.1016/j.tca.2016.11.013.

Fischer, Roland A., and Angélique. Bétard. **"Metal-Organic Framework Thin Films: From Fundamentals to Applications."** Chemical Reviews, 2011, pp. 1055–83.

Furukawa, Hiroyasu, et al. **"The Chemistry and Applications of Metal-Organic Frameworks."** Science, 2013, doi:10.1126/science.1230444.

Furukawa, Shuhei; Stephane Diring. **"Controlled Multiscale Synthesis of Porous Coordination Polymer in Nano/Micro Regimes."** Chemistry of Materials, vol. 22, no. 16, 2010, pp. 4531–38.

G.K. Williamson and W.H. Hall. **"X-Ray Line Broadening from Filled Aluminium and Wolfram."** Acta Metallurgica, vol. 1, 1953, pp. 22–31.

Israr, Farrukh, et al. "**Synthesis of Porous Cu-BTC with Ultrasonic Treatment: Effects of Ultrasonic Power and Solvent Condition.**" *Ultrasonics Sonochemistry*, vol. 29, Elsevier B.V., 2016, pp. 186–93, doi:10.1016/j.ultsonch.2015.08.023.

Kayal, Sibnath, et al. "**Green Synthesis and Characterization of Aluminium Fumarate Metal-Organic Framework for Heat Transformation Applications.**" *Materials Letters*, vol. 221, Elsevier B.V., 2018, pp. 165–67, doi:10.1016/j.matlet.2018.03.099.

Li, Zong Qun, et al. "**Ultrasonic Synthesis of the Microporous Metal-Organic Framework Cu₃(BTC)₂ at Ambient Temperature and Pressure: An Efficient and Environmentally Friendly Method.**" *Materials Letters*, vol. 63, no. 1, Elsevier B.V., 2009, pp. 78–80, doi:10.1016/j.matlet.2008.09.010.

Liao, Peisen, et al. "**Transforming HKUST-1 Metal–Organic Frameworks into Gels – Stimuli-Responsiveness and Morphology Evolution.**" *European Journal of Inorganic Chemistry*, vol. 2017, no. 19, 2017, pp. 2580–84, doi:10.1002/ejic.201700048.

Luo, Yun, et al. "**Synthesis of Cu-BTC Metal-Organic Framework by Ultrasonic Wave-Assisted Ball Milling with Enhanced Congo Red Removal Property.**" *ChemistrySelect*, vol. 3, no. 41, 2018, pp. 11435–40, doi:10.1002/slct.201802067.

Moosavi, Seyed Mohamad, et al. "**Capturing Chemical Intuition in Synthesis of Metal-Organic Frameworks.**" *Nature Communications*, vol. 10, no. 1, Springer US, 2019, pp. 1–7, doi:10.1038/s41467-019-08483-9.

Remya, V. R., and Manju Kurian. "**Synthesis and Catalytic Applications of Metal–Organic Frameworks: A Review on Recent Literature.**" *International Nano Letters*, vol. 9, no. 1, Springer Berlin Heidelberg, 2019, pp. 17–29, doi:10.1007/s40089-018-0255-1.

Sargazi, Ghasem, et al. "**Rapid Synthesis of Cobalt Metal Organic Framework.**" *Journal of Inorganic and Organometallic Polymers and Materials*, vol. 24, no. 4, 2014, pp. 786–90, doi:10.1007/s10904-014-0042-z.

Schlichte, Klaus, et al. "**Improved Synthesis, Thermal Stability and Catalytic Properties of the Metal-Organic Framework Compound Cu₃(BTC)₂.**" *Microporous and Mesoporous Materials*, vol. 73, no. 1–2, 2004, pp. 81–88, doi:10.1016/j.micromeso.2003.12.027.

Shan, Meixia, et al. "**Facile Manufacture of Porous Organic Framework Membranes for Precombustion CO₂ Capture.**" *Science Advances*, vol. 4, no. 9, 2018, pp. 1–7, doi:10.1126/sciadv.aau1698.

Stock, Norbert, and Shyam Biswas. "**Synthesis of Metal-Organic Frameworks (MOFs): Routes to Various MOF Topologies, Morphologies, and Composites.**" *Chemical Reviews*, vol. 112, no. 2, 2012, pp. 933–69, doi:10.1021/cr200304e.

Tranchemontagne, David J., et al. "**Room Temperature Synthesis of Metal-Organic Frameworks: MOF-5, MOF-74, MOF-177, MOF-199, and IRMOF-0.**" *Tetrahedron*, vol. 64, no. 36, 2008, pp. 8553–57, doi:10.1016/j.tet.2008.06.036.

Trickett, Christopher A., et al. **“The Chemistry of Metal-Organic Frameworks for CO₂ Capture, Regeneration and Conversion.”** *Nature Reviews Materials*, vol. 2, no. 8, Macmillan Publishers Limited, 2017, pp. 1–16, doi:10.1038/natrevmats.2017.45.

Valadez Sánchez, Elvia P., et al. **“ α -Al₂O₃-Supported ZIF-8 SURMOF Membranes: Diffusion Mechanism of Ethene/Ethane Mixtures and Gas Separation Performance.”** *Journal of Membrane Science*, vol. 594, no. July 2018, Elsevier B.V., 2020, p. 117421, doi:10.1016/j.memsci.2019.117421.

Xu, Hangxun, et al. **“Sonochemical Synthesis of Nanomaterials.”** *Chemical Society Reviews*, vol. 42, no. 7, 2013, pp. 2555–67, doi:10.1039/c2cs35282f.

Zhao, Xiang, et al. **“Metal–Organic Frameworks for Separation.”** *Advanced Materials*, vol. 30, no. 37, 2018, pp. 1–34, doi:10.1002/adma.201705189.